Partially Oxidized Group 3B Fluorometallophthalocyanines †

Patrick Brant,* David C. Weber, Steven G. Haupt, Ronald S. Nohr, and Kenneth J. Wynne
The Chemistry Division, Code 6100, Naval Research Laboratory, Washington, D.C. 20375, U.S.A.

The fluorine-bridged Group 3 metal phthalocyanines [{M(pc)F}$_n$] (M = Al or Ga) have been reacted with nitrosonium salts NO^+Y^- (Y = BF_4 or PF_6). Pressed pellets from the products of these reactions have conductivities as high as 10 Ω^{-1} cm^{-1}. Pellet conductivities are maintained indefinitely in ambient air. Samples are thermally stable (thermogravimetric analysis) up to *ca.* 150 °C. Thermally-ramped mass spectra show that primary decomposition products are fluorinated organic compounds and anion fragments. *X*-Ray powder diffraction data show that new diffraction lines are formed on doping these stacked polymers. It is believed that these new lines correspond to some disruption of the original crystal lattice. A broad electronic transition is detected in the i.r. spectra of the doped products; the intensity of this transition increases with increasing dopant concentration. The pure precursor phthalocyanines are diamagnetic while the doped products all contain delocalized unpaired spins. Product spin densities at room temperature, measured both by e.s.r. and magnetic susceptibility methods, are between 0.005 and 0.18 spins per dopant molecule. Spin-signal temperature dependences identified include Pauli-like behaviour with a Curie tail, and antiferromagnetic behaviour. *X*-Ray photoelectron spectra of doped products are consistent with delocalised positive charges (holes) on the phthalocyanine rings. The fluorine and boron or phosphorus core-level signals from the dopant anions are always weaker than expected from the stoicheiometry of the doped product. These weak signals are believed to be associated with the anion being located inside channels created by surrounding phthalocyanines.

We have previously reported iodine doping of polymeric [{M(pc)F}$_n$] [pc = phthalocyaninate(2−); M = Al, Ga, Cr] which gives highly conducting polymeric complexes of composition [{M(pc)FI_x}$_n$].[1,2] In addition, we have shown through a single-crystal *X*-ray structure determination that [Ga(pc)F] has the bridge-stacked polymeric structure (I).[3] In continuing the investigation of these unusual bridge-stacked phthalocyanine polymers, we have prepared and characterized BF_4^-- and PF_6^--doped [{Al(pc)F}$_n$] and [{Ga(pc)F}$_n$]. These compositions show exceptional resistance to thermal stress and are indefinitely stable in ambient air.

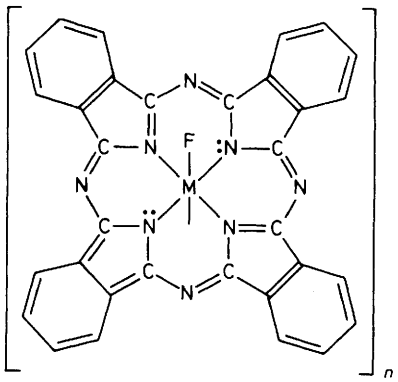

(I)

Experimental

The (polymeric) precursor phthalocyanines, [Al(pc)F] and [Ga(pc)F], were prepared and purified following established procedures.[4] Nitrosonium salts were purchased from Alfa Inorganics and stored at −10 °C prior to use. The preparative method for doping the phthalocyanines was the same in all cases. A detailed description of the procedure for moderately doping [Al(pc)F] with $NOPF_6$ will serve to illustrate the synthetic approach. In a dry-box, weighed portions of [Al(pc)F] (1.8 mmol) and dry $NOPF_6$ (0.6 mmol) along with a magnetic-stir bar were transferred to a Schlenk tube. Dry, degassed nitromethane (*ca.* 5 cm^3) was then vacuum distilled onto the reactants. The mixture was allowed to equilibrate to room temperature. Evolution of gas began soon after the solvent melted and continued for 0.5 h. After standing another 0.5 h the tube was opened to air and the product filtered twice. The product was washed with portions of nitromethane and dried *in vacuo* (yield 0.95 g, 86%). Some product was invariably lost in all preparations due to the extremely small particle size of the [Al(pc)F]. Product yields were always 80—90% (based on phthalocyanine). In some cases dry dichloromethane was used as solvent. Elemental analyses (Galbraith Analytical Labs., Knoxville, Tennessee) were obtained for some of the oxidized products. These are summarized in Table 1. Remaining [M(pc)F]: dopant (dopant = PF_6^- or BF_4^-) stoicheiometries were determined from the weights of the dry reactants or from the volume of a stock $NOPF_6$ solution added to a weighed quantity of [M(pc)F].

Products were characterized by a number of different physical methods. Infrared spectra were recorded for starting materials and products as Nujol mulls supported between KBr or NaCl plates on a Perkin-Elmer 457 or 580B spectrometer. *X*-Ray powder patterns were obtained using a Läue camera and Cu-K_α *X*-rays. Thermogravimetric analyses (t.g.a.) were recorded using a DuPont 951 controller coupled with a model 2990 thermal analyser. E.s.r. spectra of the powders were recorded at *X*-band frequency with a Bruker ER200-D spectrometer. Signal *g* values and intensities were calibrated with a standard diphenylpicrylhydrazyl (dpph) sample (g = 2.0036). Magnetic susceptibilities were determined by the Faraday method at Johns Hopkins University (Baltimore). Diamagnetic corrections were estimated using Pascal's con-

* *Present address*: P.O. Box 5200, Exxon Chemical Company, Baytown, Texas 77522, U.S.A.

† Presented in part at the International Conference on Low-dimensional Conductors, Boulder, Colorado, U.S.A., 9–14 August, 1981.

Non-S.I. units employed: G = 10^{-4} T, eV ≈ 1.60 × 10^{-19} J.

Table 1. Elemental analysis (%) [a] for $[M(pc)F(Y)_x]$

Complex	C	H	N	M	F [b]	P
$[Al(pc)F(PF_6)_{0.38}]$	64.6	2.85	18.7	4.55	7.55	1.25
	(64.1)	(2.65)	(18.7)	(4.80)	(8.50)	(1.45)
$[Al(pc)F(PF_6)_{0.59}]$	59.6	2.75	17.2	3.55	11.5	2.45
	(59.7)	(2.50)	(17.4)	(4.20)	(13.4)	(2.85)
$[Al(pc)F(BF_4)_{0.44}]$				4.55	8.80	
				(4.50)	(8.65)	
$[Ga(pc)F(PF_6)_{0.31}]$	59.5	2.70	17.3	10.9	7.45	1.55
	(59.4)	(2.50)	(17.3)	(10.8)	(8.40)	(1.50)

[a] Calculated values are in parentheses. [b] Fluorine analyses are generally deficient relative to the calculated values.

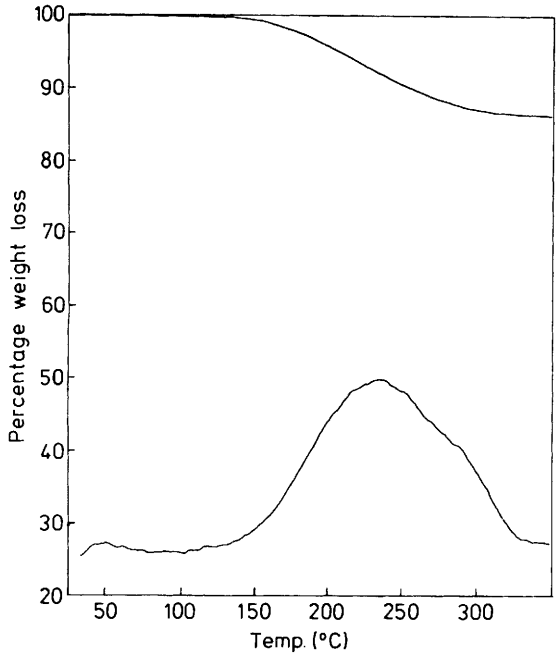

Figure 1. Thermogravimetric analysis of $[Al(pc)F(PF_6)_{0.59}]$; the upper trace is sample weight loss (as %) as a function of temperature, the lower trace is the derivative, dw/dT, of the upper trace

stants.[5] Conductivities of pressed pellets were determined by the four-point-probe van der Pauw method.[6] Mass spectra were obtained using a Hewlett-Packard 35 GC/MS spectrometer and *X*-ray photoelectron spectra (x.p.s.) were recorded using McPherson ESCA-36 and Leybold-Hereaus S-10 spectrometers.

Results and Discussion

Reaction of polymeric [Al(pc)F] and [Ga(pc)F] with $NOBF_4$ and $NOPF_6$ occurs smoothly in dry nitromethane or dichloromethane to yield materials of general composition $[M(pc)F(Y)_x]$ (for M = Al, Y = PF_6, $x_{max.} = 0.59$; Y = BF_4, $x_{max.} = 0.9$; for M = Ga, Y = PF_6, $x_{max.} = 0.66$; Y = BF_4, $x_{max.} = 0.90$). Compositions having $x_{max.}$ were obtained using excess NOY, while compositions with lower values of x could be obtained by making NOY the limiting reagent. Analytical data consistent with the proposed formulae (Table 1) were obtained on some of the first doped samples. Other subsequent compositions are based on the weights of the two reactants.

Complexes of compositions $[M(pc)F(Y)_x]$ have good thermal stability. In nitrogen, a weight-loss process for these compositions starts at *ca.* 150 °C (Figure 1). Mass spectroscopic evidence shows that in this temperature range (125—175 °C) weight loss appears to be dominated by organic fragments such as those appearing at $m/e = 147$ (100%) assigned to $C_6H_4(CN)(CNF)^+$, $m/e = 104$ assigned to $C_6H_4(CNH)^+$, and $m/e = 76$ assigned to $C_6H_4^+$. In contrast, weight loss (by t.g.a.) or fragmentation peaks (by mass spectrometry) are not observed below 400 °C for the pure unoxidized [M(pc)F]. Consequently, the initial decomposition process is believed to result from reaction between the anion and the pc ring. This is further supported by the mass spectra, which are dominated at higher temperatures by dopant ion fragmentation peaks (*e.g.* PF_m^+, $m = 1$—4) with the exception of those for PF_5^+ or BF_3^+ which are conspicuously absent.[7] The total weight loss when the temperature has reached 350 °C generally exceeds the weight of the dopant by a few per cent.

Infrared spectra for oxidized and unoxidized [Al(pc)F] are compared in Figure 2. The i.r. spectra of the doped compositions show a broad envelope of absorption centred at *ca.* 1 800 cm^{-1} (0.22 eV). This broad absorption increases in intensity with increasing dopant concentration. This low-lying electronic excitation is superimposed on and eventually obscures all but the strongest i.r. peaks. A similar, but weaker electronic band is observed in the i.r. spectra of the doped $[Ga(pc)F(Y)_x]$. These broad electronic transitions have also been observed in iodine-doped [M(pc)O] (M = Si, Ge, or Sn).[8] In all doped materials a sharp absorption characteristic of the PF_6^- ion is observed at 845 cm^{-1}. Comparable peaks for BF_4^- are not clearly seen due to a combination of the electronic excitation and pc peaks.

Compressed-pellet conductivity measurements reveal conductivities of the order of 0.2—10 Ω^{-1} cm^{-1} for the maximally BF_4^-- and PF_6^--doped materials. Lower conductivities were observed for lower doping levels. Figure 3 shows the relationship between conductivity and dopant concentration. Recent temperature-dependent conductivity studies[9] have revealed low activation energies consistent with macroscopic conductivity limited by interparticle resistance.

A remarkable feature of these materials is the invariant conductivity upon exposure to ambient air. Thus, an independent check on $[Al(pc)F(PF_6)_{0.59}]$ on a different conductivity apparatus after three months exposure to air showed the conductivity was virtually unchanged (0.2 Ω^{-1} cm^{-1}). Further, the conductivity of $[Al(pc)F(BF_4)_{0.44}]$ stored in ambient air remained unchanged (3×10^{-2} Ω^{-1} cm^{-1}) for over one year. The stability of $[M(pc)F(Y)_x]$ to thermal stress and exposure to ambient air is in contrast to the behaviour of iodine-doped [M(pc)F] and many other conducting polymers or non-metallic materials.[10-12] For example, loss of iodine is observed from $[M(pc)FI_x]$ unless the sample has been thermally pre-treated.[2]

X-Ray film powder pattern data for pure [M(pc)F] and doped products are summarized in Table 2. Results show that with doping new diffraction lines appear. Marks and co-

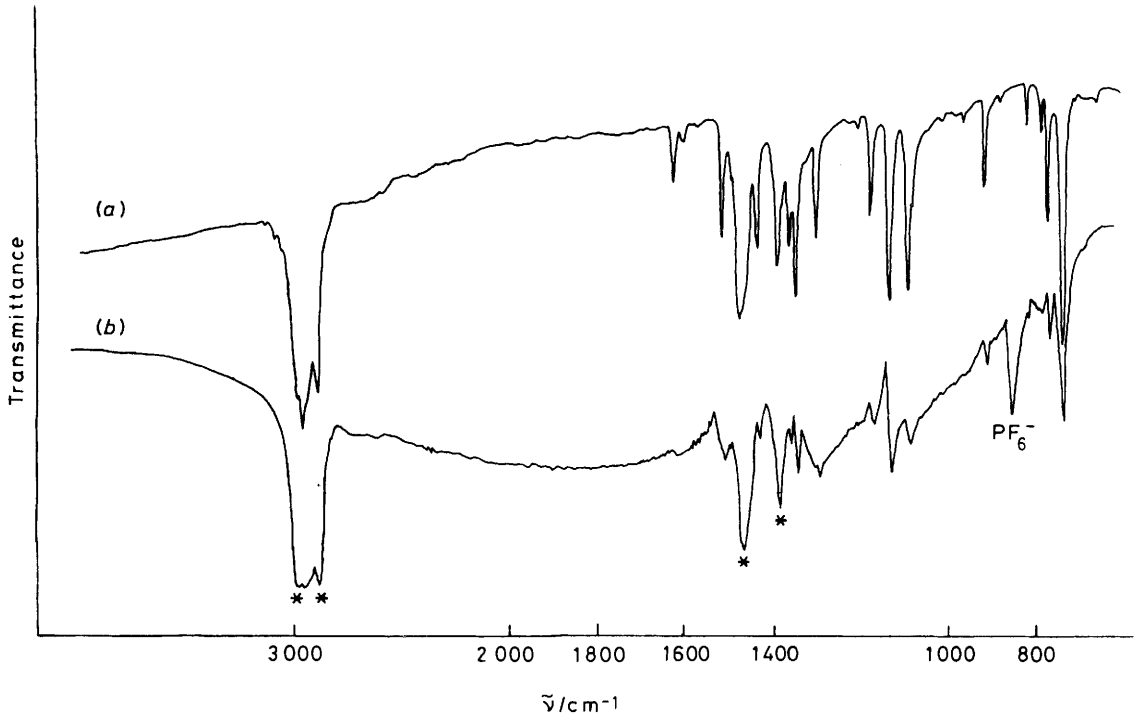

Figure 2. I.r. spectra of (*a*) pure [Al(pc)F] and (*b*) [Al(pc)F$(PF_6)_{0.38}$]. Lines denoted with an asterisk are due to mineral oil

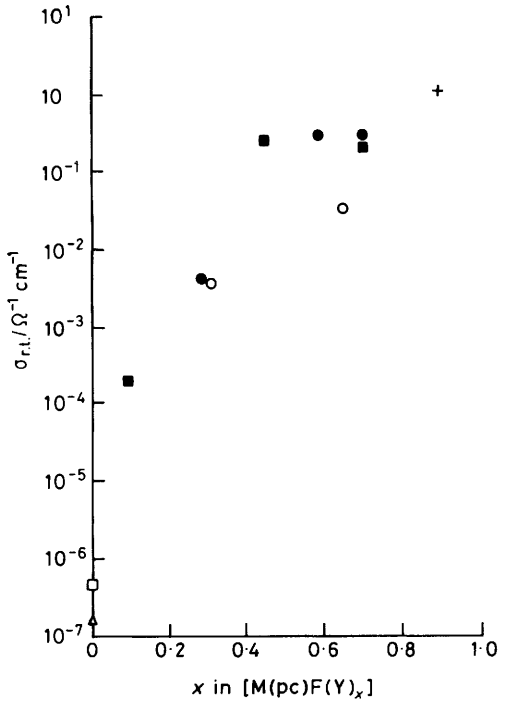

Figure 3. Pressed-pellet conductivity *versus* dopant concentration: M, Y = Al, PF_6 (●); Ga, PF_6 (○); Al, BF_4 (■); Ga, BF_4 (+). Data for pure [Al(pc)F] (□) and [Ga(pc)F] (△) are taken from ref. 2

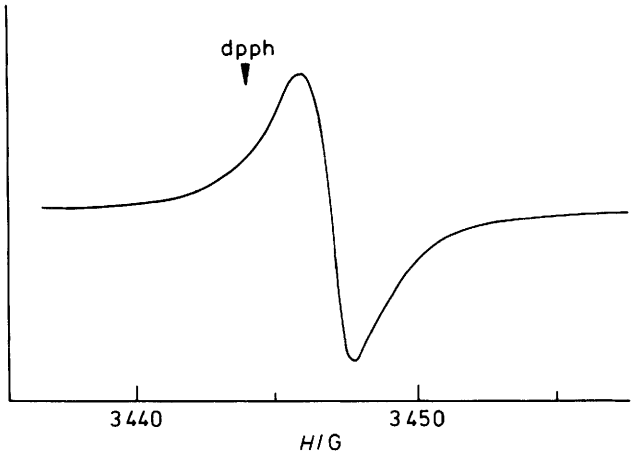

Figure 4. Room-temperature *X*-band e.s.r. spectra of [Al(pc)-F$(PF_6)_{0.59}$]. Frequency modulation 100 kHz, modulation amplitude 0.8 G

workers [8] reported new diffraction lines which increase with increasing iodine dopant concentration for the [M(pc)O] systems (M = Si, Ge, or Sn). The nature of these new structural forms is not presently known.

All of the [M(pc)F$(Y)_x$] materials exhibit e.s.r. spectra which show a single narrow, nearly symmetric absorption with *g* very close to the free-electron value. A typical spectrum is shown in Figure 4. Room-temperature signal parameters are summarized in Table 3. Peak-to-peak linewidths are between 0.3 and 2.6 G and the signals are all strongly Lorentzian in shape. No e.s.r. signal is found in the neutral [M(pc)F] polymers.

The number of unpaired spins generated per added BF_4^- or PF_6^- ion has been independently determined by e.s.r. and magnetic susceptibility measurements and was found to be between 0.005 and 0.18. Initially there appeared to be no correlation between spin density and dopant concentration. However, these comparisons involved different dopants (BF_4^- and PF_6^-), different metals (Al and Ga), and different solvents (CH_2Cl_2 and CH_3NO_2). Consequently, a more controlled experiment was performed in which all independent

Table 2. Powder diffraction data (d spacings/Å) for some [M(pc)F(Y)$_x$] complexes

Complex								
[Al(pc)F]		3.55 (m)	3.66 (s)					13—15 (s)
[Al(pc)F(PF$_6$)$_{0.38}$]	1.84 (w)		3.62 (s)		5.38 (m)	6.4 (w)		13 (s)
[Al(pc)F(PF$_6$)$_{0.59}$]		3.4 (w)	3.55 (s)	4.65 (m)		6 (w)	9.6 (s)	
[Ga(pc)F]		3.70 (m)	3.86 (s)					
[Ga(pc)F(PF$_6$)$_{0.42}$]		3.70 (s)	3.85 (m)		5.6 (m)		9.5 (m)	13 (vs)

Table 3. Room-temperature magnetic properties of [M(pc)F(Y)$_x$] (M = Al or Ga, Y = BF_4 or PF_6) and [M(pc)F]

	E.s.r. parameters			Unpaired spins per [M(pc)F] unit	
Complex	g value [a]	Linewidth (G)	A/B [b]	M.s. [c]	E.s.r. [d]
[Al(pc)F]					0
[Al(pc)F(PF$_6$)$_{0.38}$]	2.0024	0.62	0.94	0.0012	0.006
[Al(pc)F(BF$_4$)$_{0.44}$]	2.0025	1.30	0.94		0.035
[Al(pc)F(PF$_6$)$_{0.59}$]	2.0028	1.71	0.96		0.18
[Ga(pc)F]					0
[Ga(pc)F(PF$_6$)$_{0.10}$]	2.0024	2.6	0.94		0.07
[Ga(pc)F(PF$_6$)$_{0.31}$]	2.0025	1.2	0.97	0.091	0.11
[Ga(pc)F(PF$_6$)$_{0.30}$]	2.0025	2.6	0.91		0.013
[Ga(pc)F(PF$_6$)$_{0.60}$]	2.0025	2.4	0.99		0.020
[Ga(pc)F(BF$_4$)$_{0.9}$]	2.0025	0.35	0.93		0.010

[a] Determined using dpph calibrant. [b] Peak symmetry measurement: ratio of heights of positive and negative deflections in derivative signal. [c] Magnetic susceptibility: diamagnetic corrections made using Pascal's constants. [d] Spins measured using dpph calibrant.

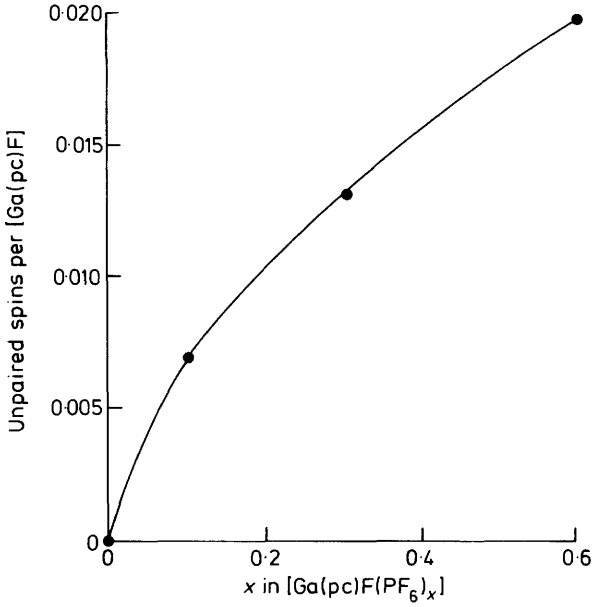

Figure 5. Unpaired spins generated as a function of dopant concentration for the reaction of [Ga(pc)F] with appropriate volumes of a stock solution of 0.05 mol dm^{-3} $NOPF_6$ in nitromethane

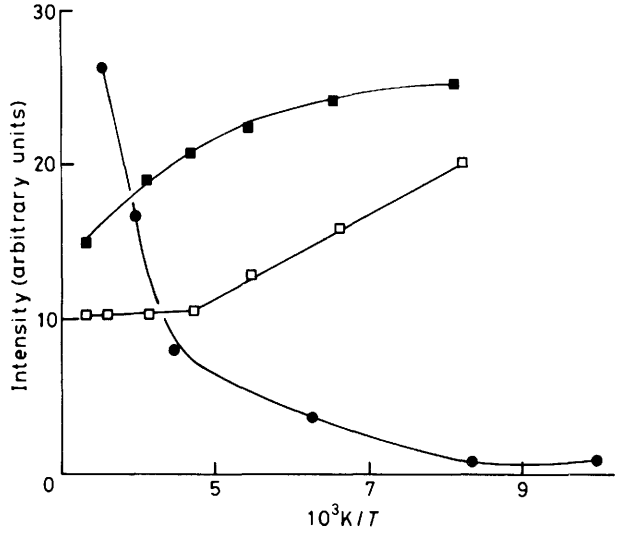

Figure 6. E.s.r. signal intensity *versus* $1/T$ for [Ga(pc)F(BF$_4$)$_{0.9}$] (■), [Ga(pc)F(PF$_6$)$_{0.9}$] (□), and [Al(pc)F(PF$_6$)$_{0.38}$] (●)

variables were held constant except for the dopant concentration. The experiment was executed in the following manner. A stock solution of 0.05 mol dm^{-3} $NOPF_6$ in CH_3NO_2 was prepared. Equal weights of [Ga(pc)F] were placed into three separate dry e.s.r. tubes. In a dry-box, a portion of the stock solution was added to each tube. When the doping reaction was complete the tubes were transferred to a vacuum line and the CH_3NO_2 solvent slowly removed under reduced pressure. The samples were then removed from the line and the e.s.r. spectra immediately recorded. Spin densities are plotted *versus* added dopant in Figure 5. Here we observe a smooth (possibly linear, given experimental errors) increase in spin density with dopant concentration. Assuming the relationship to be linear the slope of the plot is roughly 0.05 unpaired electron per added PF_6^-.

The low spin concentrations per added dopant ion could be a consequence of Pauli paramagnetism. Marks and co-workers [8] have interpreted their magnetic susceptibility measurements for iodine-doped [M(pc)O] systems in just this way. However, their variable-temperature susceptibility measurements are complicated by 'skewing' to large susceptibilities at low temperatures. This skewing was attributed to paramagnetic impurities formed in the doping procedure.

We have used e.s.r. instead of magnetic susceptibility to investigate the spin signal dependence on temperature. Three doped products have been examined. These measurements are

Table 4. *X*-Ray photoelectron spectroscopic data (eV) [a] for some doped and pure [M(pc)F] complexes

Complex	Al 2*p*	N 1*s*	C 1*s* [b]	F 1*s*	F/N Ratio: Expected [c]	F/N Ratio: Found [d]
[Al(pc)F]	74.5 (1.5)	398.6 (1.5)	284.4 (2.3)	685.4 (1.8)	0.125	0.14
[Al(pc)F$(PF_6)_{0.38}$]	74.6 (1.6)	398.5 (1.6)	284.4 (2.2)	685.5 (2.2)	0.41	0.33
[Al(pc)F$(PF_6)_{0.59}$]	74.6 (1.7)	398.4 (1.7)	284.4 (2.2)	685.6 (1.8)	0.57	0.27
	Ga $3p_{3/2}$					
[Ga(pc)F]	1 117.7 (1.4)	398.8 (1.7)	284.4 (2.2)	684.3 (1.8)	0.125	0.12
[Ga(pc)F$(PF_6)_{0.3}$]	1 117.8 (1.3)	398.6 (1.5)	284.4 (2.1)	685.8 (1.9)	0.35	0.30
[Ga(pc)F$(PF_6)_{0.42}$]	1 118.0 (1.5)	398.7 (1.3)	284.4 (1.9)	685.9 (2.1)	0.44	0.40
[Ga(pc)F$(PF_6)_{0.70}$]	1 117.7 (1.4)	398.5 (1.5)	284.4 (2.0)	685.6 (2.0)	0.65	0.51
[Ga(pc)F$(BF_4)_{0.9}$]	1 117.6 (1.6)	398.6 (1.7)	284.4 (2.2)	685.5 (1.9)	0.575	0.42

[a] Values in parentheses are peak full-widths at half-maxima, in eV. [b] All binding energies referenced to C 1*s* of 284.4 eV. [c] Based on elementa analyses or weights of reactants. [d] Determined from core-level peak intensities.

plotted in Figure 6. For our systems and doping procedures, the signal dependence with temperature can vary dramatically. For example, the heavily doped composition [Ga(pc)F-$(PF_6)_{0.6}$] gives an e.s.r. signal intensity dependence in keeping with those reported by Marks and co-workers [8] for the iodine-doped [M(pc)O] systems (M = Si or Ge): namely Pauli-like behaviour with a strong Curie tail.

The [Al(pc)F$(PF_6)_{0.38}$] sample gave an entirely different result. Here we encountered temperature-dependent behaviour characteristic of strong antiferromagnetic coupling between electrons. This behaviour was so surprising that it has been examined twice and the curve generated both with incrementally increasing and decreasing temperatures. The general curve shape is always reproduced although some hysteresis is observed. The simplest explanation for this result might be spin correlation of unpaired electrons on adjacent [M(pc)F] units strung together over some undetermined length.

Other features of the e.s.r. spectra are also worth noting. First, we found that the derivative signal e.s.r. linewidths (peak-to-peak) vary from being independent of temperature, as is the case for [Ga(pc)F$(BF_4)_{0.9}$], to being substantially broadened at low temperature.

In all cases, the A/B ratio (Table 3) of the derivative e.s.r. signals is between 0.91 and 0.99. There is no correlation of this ratio with dopant concentration. The slight signal distortion probably derives from slight differences in $g_{\parallel}$ and $g_{\perp}$, although sample skin depth may be a factor. If skin depth is a factor here, the intrinsic microcrystal conductivity at microwave frequencies would have to be in excess of *ca.* 700 Ω^{-1} cm^{-1}.*

X-Ray photoelectron spectra were recorded for the neutral and a variety of the doped compositions of the fluorometallophthalocyanines and the data are presented in Table 4. The nitrogen 1*s* spectra of both the neutral and doped species exhibit single, slightly asymmetric lines consistent with roughly equivalent environments of the eight pyrollic nitrogens. Oxidation results in at most a 0.1—0.2 eV decrease in the N 1*s* binding energy relative to the C 1*s* line. Carbon 1*s* spectra of the neutral [M(pc)F] materials consist of three peaks with an overall envelope shape very nearly the same as that reported by Verbist and co-workers[13] for [Fe(pc)] monomer. The strongest, lowest-binding-energy peak is from the phenyl ring carbons. The next strongest peak, at 1.7 eV higher energy than the first, is from the pyrollic carbons. This relationship is established by the relative peak intensities. Additionally, there is a satellite separated by 3.3 eV from the largest peak. Verbist and co-workers [13] have already proposed that this satellite corresponds to an $e_g(\pi)$ to $e_g(\pi^*)$ phthalocyanine-centred transition and we concur with this assignment. The intensity between satellite and main lines is conserved and the overall envelope shape is retained on doping (oxidation) but envelope definition deteriorates progressively with higher doping levels.

The central metal core-level lines are sharp and their definition and binding energies are unchanged by doping. All of these observations complement our e.s.r. results from which we know that unpaired electrons in the doped products reside in highly delocalized orbitals. From x.p.s. we conclude that the positive charge introduced onto the phthalocyanine rings by each dopant molecule is shared equally among the ring (benzenic and pyrollic) atoms.

The F 1*s* binding energies of the bridging fluoride ions in the neutral [M(pc)F] compounds are at 685.4 (M = Al) and 684.3 eV (M = Ga). The lower F 1*s* binding energy for the gallium polymer arises from the lower electronegativity and greater polarizability of the Ga^{III} ion compared with Al^{III}.

On doping these polymers we might expect to see two F 1*s* peaks where the intensities of the two peaks reflect the quantity of dopant added. Such doublet spectra are expected because the BF_4^- and PF_6^- fluorine 1*s* binding energies are in the range 685.8 and 686.1 eV respectively.[14,15] These expectations have not been fully achieved in any of the doped products yet examined. The F 1*s* spectra which should give the best doublet resolution are shown in Figure 7. In these and all other spectra we find first that the quantity of fluorine detected is substantially less than that which is known to be contributed from the dopant ion (by elemental analysis and gravimetric methods). The quantities detected from integrated peak intensities are often lower than the quantities expected by 20—40%. Correspondingly high intensity debits of 30—50% are registered for the P 2*p* and B 1*s* signals. Although the signals are weak, at the highest doping levels there appears to be more than one P or B environment. The expected fluorine 1*s* doublets are, with few exceptions, very poorly defined. Often, there is only a single broad F 1*s* line, even for [Ga(pc)F] doped with $NOPF_6$ where the F 1*s* binding-energy difference of 1.8 eV between bridging fluoride ions and PF_6^- fluorine ions should result, as can be shown by curve simulations, in two reasonably well resolved peaks.

The substantial discrepancies between expected and observed dopant-anion spectra are believed to have two causes. First, we know from the mass spectral data that small quantities of fluorinated by-products are created in the doping reaction. By-product concentrations may be further enhanced

* This conductivity is based on the following classical relationship between sample conductivity and skin depth: $S = c(2\sigma w)^{\frac{1}{2}}$, where S is the skin depth, c the speed of light, σ the d.c. conductivity, and w the frequency of the incident light. Distortion of the e.s.r. signal will occur when S approaches the dimensions of the crystallites (*ca.* 0.01 × 0.01 × 0.2 mm columns for our samples).

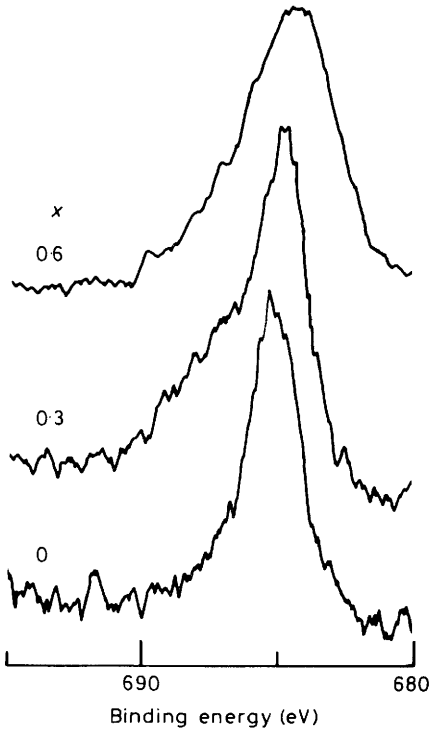

Figure 7. Fluorine 1*s* spectra of $[Ga(pc)F(PF_6)_x]$

under the conditions of the x.p.s. data collection. These products diminish the resolution and change expected intensity relationships of F 1*s* spectra. Secondly, and most likely, the diminished anion spectra may simply result from energy minimization in the solid state. It is possible that the lowest-energy position for the 'hard-sphere' anions is inside the cylindrical channels which we know can exist in some representative phthalocyanines and which can also be retained in doped products.[16] If this is the case, then the dopant anions are always surrounded by the massive phthalocyanine rings which are 13 Å across. This phthalocyanine overlayer will attenuate the dopant-anion signals to the following extent:[17] $I/I_0 = e^{-d/\lambda}$, where d is the overlayer thickness and λ is the inelastic mean free path of the appropriate photoelectron. For $d = 13$ Å (approximate diameter of phthalocyanine ring) and $\lambda = 20$ Å (ref. 18) the expected signal intensity, I_0, will be reduced 48%. We believe the diminished anion spectra are largely due to the preferential placement of the dopant anions in the large channels or spaces between phthalocyanine stacks.

Conclusions

We have shown that the [M(pc)F] (M = Al or Ga) compositions can be chemically doped with nitrosonium salts to yield air- and thermally-stable products with high compacted powder conductivities. An electronic transition centred in the i.r. (0.22 eV) is prominent in moderate to heavily oxidized products but the transition appears to be too energetic to be associated with the conductor pathway. We know that charge transport has an activation energy of only 0.003 eV and this barrier is most likely associated with interparticle contact resistance.

Mass and i.r. spectra, and elemental analyses show that the BF_4^- and PF_6^- ions introduced by reactions with the nitrosonium salts are largely intact in the doped products. E.s.r. and magnetic susceptibility measurements establish that the undoped compounds are diamagnetic whereas the doped products contain between 0.005 and 0.18 unpaired spins per dopant anion. Careful doping experiments using the same reaction system (phthalocyanine, dopant, solvent) show that the number of unpaired spins created increases approximately linearly with dopant concentration. The large variation in spins per dopant anion is believed to arise largely from creation of varying quantities of paramagnetic impurities during the doping reaction. The unpaired electrons in the doped products are delocalized. Spectra recorded at temperatures as low as 4 K have failed to resolve any hyperfine splittings although in most cases the lower temperatures significantly broaden the signal. *X*-Ray photoelectron spectroscopy shows the positive charges introduced by the dopant oxidation are delocalized over the conjugated phthalocyanine rings. Dopant core-level spectra are diminished 20—40% in intensity and have poorer than expected resolution. The most likely reasons for this result are that these spectra are selectively attenuated because the BF_4^- and PF_6^- anions reside in cavities surrounded by the large phthalocyanine rings and small amounts of fluorinated organic by-products broaden the F 1*s* envelope.

Acknowledgements

We thank Dr. Wayne Bridon of Johns Hopkins University (Baltimore, Maryland) for making the magnetic susceptibility measurements on the doped polymers and Drs. Gerry Chingas and Dale Pace for use of the e.s.r. spectrometer.

References

1 P. M. Kuznesof, K. J. Wynne, R. S. Nohr, and M. E. Kenney, *J. Chem. Soc., Chem. Commun.*, 1980, 121.
2 R. S. Nohr, P. M. Kuznesof, K. J. Wynne, M. E. Kenney, and P. G. Siebenman, *J. Am. Chem. Soc.*, 1981, **103**, 4371.
3 R. S. Nohr and K. J. Wynne, *J. Chem. Soc., Chem. Commun.*, 1981, 1210.
4 J. P. Linsky, T. R. Paul, R. S. Nohr, and M. E. Kenney, *Inorg. Chem.*, 1980, **19**, 3131.
5 E. Konig, 'Magnetic Properties of Coordination and Organometallic Compounds of the Transition Elements,' Springer-Verlag, Berlin, 1965.
6 L. J. van der Pauw, *Philips Res. Rep.*, 1958, **13**, 1.
7 F. E. Saalfeld, J. J. Decorpo, J. R. Holtzclaw, J. Wyatt, P. Brant, and D. C. Weber, *Int. J. Mass Spectrom. Ion Phys.*, 1981, **40**, 101.
8 B. N. Diel, T. Inabe, J. W. Lyding, K. F. Schoch, C. R. Kannewurf, and T. J. Marks, *J. Am. Chem. Soc.*, 1983, **105**, 1551.
9 D. C. Weber and P. Brant, unpublished work.
10 C. K. Chiang, M. A. Druy, S. C. Gau, A. J. Heeger, E. J. Louis, A. G. MacDiarmid, Y. W. Park, and H. Shirakawa, *J. Am. Chem. Soc.*, 1978, **100**, 1013.
11 J. M. Pochan, D. F. Pochan, and H. W. Gibson, *Polymer*, 1980, **21**, 250.
12 C. M. Mikulski, P. J. Russo, M. S. Saran, A. G. MacDiarmid, A. F. Garito, and A. J. Heeger, *J. Am. Chem. Soc.*, 1975, **97**, 6358.
13 S. Maroie, M. Savy, and J. J. Verbist, *Inorg. Chem.*, 1979, **18**, 2560.
14 P. Brant, L. S. Benner, and A. L. Balch, *Inorg. Chem.*, 1979, **18**, 3422.
15 P. Brant, H. D. Glicksman, D. J. Salmon, and R. A. Walton, *Inorg. Chem.*, 1978, **17**, 3203.
16 C. S. Schramm, R. P. Scaringe, D. R. Stojekovic, B. M. Hoffman, J. A. Ibers, and T. J. Marks, *J. Am. Chem. Soc.*, 1980, **102**, 6702.
17 V. I. Nefedov, *Surf. Interface Anal.*, 1981, **3**, 72.
18 D. R. Penn, *J. Electron Spectrosc. Relat. Phenom.*, 1976, **9**, 29.

Received 25th April 1984; *Paper* 4/679